

# A Joint Temperature, Humidity, Ozone, and SST Retrieval Processing System for IASI Sensor Data: Properties and Retrieval Performance Analysis

Marc Schwaerz and Gottfried Kirchengast

*Wegener Center for Climate and Global Change (WegCenter) and  
Institute for Geophysics, Astrophysics, and Meteorology (IGAM),  
University of Graz, Graz, Austria*

## Abstract

We show the improved performance of a joint retrieval algorithm of temperature, humidity, ozone, and SST (more precisely, the latter is the surface skin temperature of the ocean) compared to more specific retrieval setups. The joint algorithm was developed based on optimal estimation methodology and carefully tested under quasi-realistic conditions (using high resolution ECMWF analysis fields). The algorithm contains in a first step an effective and fast channel selection method based on information content theory, which leads to a reduction of the total number of IASI channels ( $>8400$ ) to about 3.5% only ( $\sim 300$ ), which are subsequently used in the retrieval processing. We show that this reduction is possible without retrieval performance decrease compared to using many more ( $\sim 2000$ ) channels. Additionally, it is shown that using standard climatology fields in the channel selection process does also not decrease performance while significantly increasing computational efficiency. Finally, the application and real-data-test of the algorithm with AIRS (Advanced Infrared Sounder) data, a next step planned, is addressed.

## Introduction

The IASI (Infrared Atmospheric Sounding Interferometer) instrument will be part of the core payload of the METOP series of polar-orbiting operational meteorological satellites currently prepared for EU-METSAT (first satellite to be launched in 2006). IASI is a Michelson type Fourier transform interferometer which samples a part of the infrared spectrum contiguously from  $645\text{ cm}^{-1}$  to  $2760\text{ cm}^{-1}$  ( $\sim 15.5\text{ }\mu\text{m}$  -  $3.6\text{ }\mu\text{m}$ ) with an unapodized spectral resolution of  $0.25\text{ cm}^{-1}$ . Compared to existing operational satellite radiometers, this high spectral resolution instrument allows significantly improved accuracy and vertical resolution of retrieved temperature and humidity profiles, and also delivers ozone profiles and sea surface temperature (SST). The instrument is also designed for detection of additional trace gases and improved cloud characterization.

In this study, simulated IASI measurements are used to estimate temperature and humidity profiles and the surface skin temperature. We used the fast radiative transfer model RTIASI for forward modeling and simulating the IASI measurements (see subsection *Forward Modeling*). Due to performance and numerical reasons a fast channel selection method based on information content theory, which leads to a reduction of the total number of IASI channels ( $>8400$ ) to about 3.5% only ( $\sim 300$ ), is introduced in the subsection *Channel reduction procedure*. The retrieval of the atmospheric variables is prepared by following the Bayesian approach for an optimal combination of *a priori* data and new measurements using a fast converging iterative optimal estimation algorithm (Rodgers, 2000) (see subsection *Retrieval Algorithm*).

The retrieval algorithm is then applied to a quasi realistic METOP/IASI orbit track for September 15, 2002. Results for this case study are presented in the section *Results*. A summary of the work presented as well as suggested improvements and future steps on the IASI retrieval problem are given in the section *Summary and Outlook*.

## Data Simulation and Retrieval Methodology

This section briefly describes the retrieval scheme, the forward modeling involved, the main aspects of the retrieval algorithm itself, and the procedure of information content based channel reduction. The description follows (Lerner et al., 2002), and (Weisz et al., 2003) and more details can be found there. Those earlier studies used the same methodology as applied here but were linked to the development of single parameter (temperature-only and humidity-only) retrieval schemes.

### Forward Modeling

For a successful retrieval of atmospheric parameters within the framework of an optimal estimation approach as adopted here, the underlying physics of the measurement needs to be properly modeled by a forward model solving the radiative transfer equation. At the same time, a proper modeling of the "Jacobian matrix" (also termed "weighting function matrix", i.e., the derivative of the forward model with respect to the state vector) is quite important, especially with regard to computational efficiency, since (moderate) non-linearities in the problem of interest demand an iterative state estimation.

For simulating the measurement vector and calculating  $\mathbf{F}(\mathbf{x}) = \mathbf{T}_B$  ( $\mathbf{T}_B$ : brightness temperature) and the Jacobians  $\mathbf{K} = \partial\mathbf{F}(\mathbf{x})/\partial\mathbf{x}$ , the fast radiative transfer model RTIASI (Matricardi and Saunders, 1999) was used, which uses temperature, humidity, and ozone profiles and some surface parameters (e.g., surface skin temperature, surface air temperature, etc.) as input and then furnishes simulated IASI brightness temperature measurements and Jacobians of the input atmospheric species for any desired subset of IASI channels. This model calculates level-to-space transmittances on 43 fixed pressure levels spanning from 0.1 hPa (~65 km height) to surface. We used these same levels, the so called "ATOVS pressure level grid", also as our retrieval grid (all 43 levels for temperature, the lowest 28 levels for humidity).

### Retrieval Algorithm

The inverse problem associated with equation  $\mathbf{y} = \mathbf{F}(\mathbf{x}) + \epsilon$ , i.e., the retrieval of temperature, humidity, and ozone profiles and of SST,  $\mathbf{x}$ , from brightness temperature measurements,  $\mathbf{y}$ , is approached by the concept of Bayesian optimal estimation described in detail by (Rodgers, 2000). With the assumption of Gaussian probability distributions and a linearized forward model, we choose a fast converging iterative optimal estimation algorithm (Rodgers, 2000):

$$\mathbf{x}_{i+1} = \mathbf{x}_{ap} + \mathbf{S}_i \mathbf{K}_i^T \mathbf{S}_\epsilon^{-1} [(\mathbf{y} - \mathbf{y}_i) + \mathbf{K}_i(\mathbf{x}_i - \mathbf{x}_{ap})], \quad (1)$$

where the subscript  $i$  is the iteration index.  $\mathbf{x}_{i/i+1}$  and  $\mathbf{x}_{ap}$  are the iterated and *a priori* state vectors, respectively ( $\mathbf{T}$ ,  $\ln \mathbf{q}$ , and SST combined in one state vector), and  $\mathbf{S}_i$  is the retrieval error covariance matrix, defined by:

$$\mathbf{S}_i = [\mathbf{S}_{ap}^{-1} + \mathbf{K}_i^T \mathbf{S}_\epsilon^{-1} \mathbf{K}_i]^{-1}. \quad (2)$$

Here  $\mathbf{S}_{ap}$  is the *a priori* error covariance matrix. The optimization scheme expressed by equation (1) is usually termed the Gauss-Newton method and provides a reliable maximum *a posteriori* estimate for "small residual" inverse problems as the one dealt with here (Rodgers, 2000). In applying equation (1), the iteration was initialized with  $\mathbf{x}_0 = \mathbf{x}_{ap}$  and state estimate  $\mathbf{x}_i$ , measurement estimate  $\mathbf{y}_i = \mathbf{F}(\mathbf{x}_i)$ , weighting function matrix  $\mathbf{K}_i = \partial\mathbf{F}(\mathbf{x})/\partial\mathbf{x}|_{\mathbf{x}=\mathbf{x}_i}$ , and retrieval error covariance estimate  $\mathbf{S}_i$ , were updated at each iteration step  $i$  until convergence was reached.

Dependent on the quality of the *a priori* profile, the first or the first two steps may need special aid with convergence due to linearization errors, which is often dealt with in extending the Gauss-Newton

scheme to the Levenberg-Marquardt scheme (Rodgers, 2000; Rieder and Kirchengast, 1999). We utilized the more simple but for the present purpose equivalently effective extension introduced by (Liu et al., 2000) termed the "D-rad" method. This method leaves equation (1) unchanged, just  $\mathbf{S}_\epsilon$  is modified in its diagonal according to:

$$\mathbf{S}_\epsilon(n, n) = \max \left[ \frac{(\mathbf{y}(n) - \mathbf{y}_i(n))^2}{\alpha}, \sigma^2(n) \right] \quad (3)$$

where  $i$  is the iteration index,  $\mathbf{y}(n)$  is the measurement value of channel  $n$ ,  $\mathbf{y}_i(n) = F_n(\mathbf{x}_i)$  is the forward modeled measurement,  $\alpha$  is a (free) control parameter set to 4 for this study, and  $\sigma^2(n)$  is the variance of the measurement noise for channel  $n$  (the original  $\mathbf{S}_\epsilon(n, n)$  values). (Liu et al., 2000) found the "D-rad" extended Gauss-Newton algorithm to perform equally well or better than the Levenberg-Marquardt algorithm in aiding convergence when a poor initial guess profile was given.

### A Priori error Covariance Matrix

For the elements of  $\mathbf{S}_{ap}$  we used an auto-regressive model variant and adopted  $\mathbf{S}_{ap}$  to be non-diagonal such that there exists inter-level correlation and the non-diagonal components fall off exponentially from the diagonal, i.e.:

$$\mathbf{S}_{ap}(i, j) = \sigma_i \sigma_j \exp \left[ -\frac{|z_i - z_j|}{L} \right], \quad (4)$$

where  $\sigma_i$  and  $\sigma_j$  are the standard deviations at height (log pressure) levels  $z_i$  and  $z_j$ , respectively, and  $L$  is the correlation length.  $L$  was set to 6 km for temperature, to 3 km for humidity, and to 10 km for ozone and the standard deviation settings are specified in Table 1. The shape of the curves was set in this way to approximately satisfy the ECMWF standard deviations for temperature and humidity; for ozone a fixed value of 20 % over the whole RTIASI pressure range was used to obtain appreciable errors since we created the ozone data out of the "true" data via perturbing them consistently with the *a priori* error covariance matrix (c. f. (Rodgers, 2000)) because the daily variations which are obtained from the ECMWF model are quite small (as seen in inspecting the rms values of ozone of the 24 h forecast field with respect to the corresponding analysis field).

<b>A priori profiles consistent with the a priori error covariance matrix</b>					
Pressure [hPa]	0.10	1.50	10.00	1013.25	SST, SAT
Error [K]	4.00	4.00	1.50	1.50	1.50
Humidity					
Pressure [hPa]	100.00	200.00	400.00	1013.25	
Error [%]	10.00	60.00	60.00	20.00	
Ozone					
Pressure [hPa]	0.10		1013.25		
Error [K]	20.00		20.00		

Table 1: Standard deviation values versus pressure values for temperature, humidity, and ozone (the values between this levels are obtained via linear interpolation in log space).

### Measurement Error Covariance Matrix

In order to create an appropriate (and consistent) measurement error covariance matrix  $\mathbf{S}_\epsilon$ , we assumed the squared IASI 1c noise values (obtained from Peter Schluessel, EUMETSAT, personal communications, 2000) to be the diagonal elements. Since they are specified at a reference temperature  $T_r = 280$  K the values are modified according to the actual brightness temperature, based on the Planck law (c. f., (Weisz et al., 2003)).

Finally the temperature modified 1c noise values are superposed with an 0.2 K forward model error value to roughly account for errors in the forward model (Collard, 1998), (J. Eyre, The Met. Office, personal communications 2000). The impact of the RTIASI forward model error on the IASI retrieval

accuracy is described in (Sherlock, 2000). Fig. 1 shows the raw IASI 1c noise values and the modified values, according to a brightness temperature calculated for the U.S. standard mid-latitude summer profile.

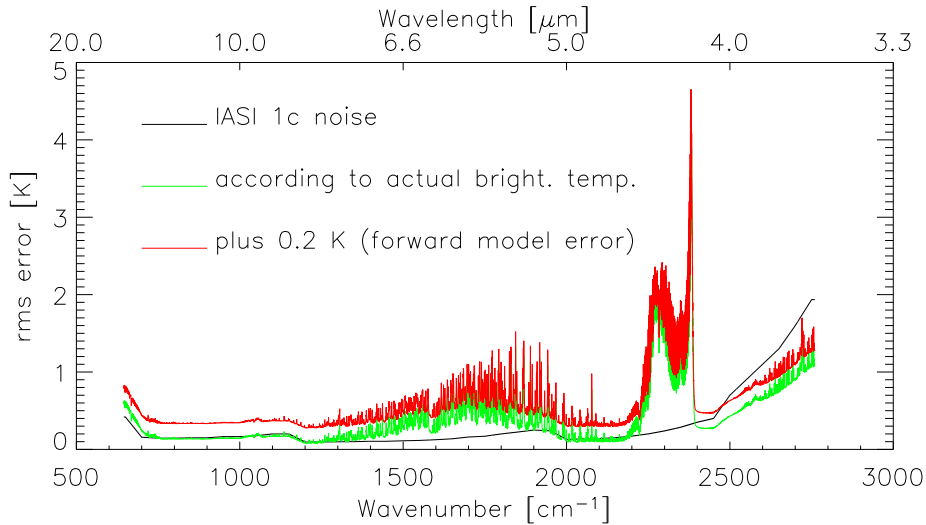


Figure 1: Square roots of the diagonal elements of the measurement error covariance matrix  $\mathbf{S}_\epsilon$ .

For the off-diagonal elements we assume a correlation  $c_{ij}$  between the three nearest neighboring channels of 0.71, 0.25, and 0.04, according to  $S_{ij} = c_{ij} \sqrt{S_{ii}S_{jj}}$ , which we also have to account for in  $\mathbf{S}_\epsilon$ . This produces an error covariance matrix with a rather steep descent from the main diagonal (Peter Schluessel, EUMETSAT, personal communications, 2000).

### Simulation of the measurement vector

Since we do not have true measurements, we add a random noise factor  $\Delta\mathbf{y}$  to the simulated measurements in order to generate quasi realistic data. For the noise modeling (receipt obtained from Peter Schluessel, personal communications, 2000) we first create normally distributed random numbers with standard deviation values according to the diagonal elements of the measurement error covariance matrix. Since RTIASI calculates apodized radiances and brightness temperatures, respectively, we apodize this noise with a Gaussian function of a full width at half maximum of  $0.5 \text{ cm}^{-1}$  ( $\sigma = 0.212 \text{ cm}^{-1}$ ).

### Channel Reduction Procedure

Since the full IASI spectra contain 8461 channels it is essential to reduce this number and somehow remove redundant information for computational and performance reasons. Hence, our task is to find a subset of channels which is sufficiently sensitive to the retrieved variables. Therefore we remove the channels above  $2500 \text{ cm}^{-1}$  (spectral range  $< 4 \mu\text{m}$  – here residual solar contribution becomes important) and those channels whose "foreign" gas emissions contribute significantly to the measured brightness temperature (i.e.,  $1220 \text{ cm}^{-1} - 1370 \text{ cm}^{-1}$  and  $2085 \text{ cm}^{-1} - 2200 \text{ cm}^{-1}$ ). At this point we have still about 6200 channels, which is still too much for our purpose.

Therefore we perform a further reduction of the number of channels by utilizing two different methods: the information content theory and the maximum sensitivity approach.

In information content theory (e. g., (Rodgers, 2000)) one seeks to know how much information is contained in a possible outcome by knowing it. If we select the channels sequentially by retaining the channels with highest information content (H) and removing them from subsequent calculations, we may write:

$$H_i = \frac{1}{2} \log_2 |\mathbf{S}_{i-1} \mathbf{S}_i^{-1}|, \quad (5)$$

where  $\mathbf{S}_{i/i-1}$  is the retrieval error covariance matrix. For  $\mathbf{S}_0$  the *a priori* error covariance matrix  $\mathbf{S}_{ap}$  was used.

As a simplified and faster alternative of using information content theory we can also use an approach, which is solely based on the weighting function matrix scaled by the measurement errors (c. f. (Weisz et al., 2003)). It is desirable to selectively choose those channels whose instrument noise is small or the measurement sensitivity to temperature and humidity perturbation is high. This is achieved by using the following channel selection criterion which maximizes the sensitivity-to-error ratio, a matrix denoted by  $\mathbf{H}$ :

$$\mathbf{H} = \mathbf{S}_\epsilon^{-\frac{1}{2}} \mathbf{K}, \quad (6)$$

where  $\mathbf{S}_\epsilon$  is again the measurement error covariance matrix (with dropping the non-diagonal elements for this purpose) and  $\mathbf{K}$  is the Jacobian Matrix.

## Results

The algorithm was tested for a quasi-realistic orbit of METOP with a full swath of the IASI instrument (more than 22000 profiles) with an ECMWF analysis field of September 15, 2002, 12 UTC, as "true" field, the 24h forecast of this analysis as first guess for temperature and humidity, and data consistent with the *a priori* error covariance matrices for ozone profiles and SST as first guess for ozone and SST, respectively (method see e. g., (Rodgers, 2000)).

The orbit ranges from Africa over Antarctica, the Pacific Ocean and the Arctic region back to Africa via eastern Europe. The red line delineates the suborbital track of the METOP satellite (see Fig. 2).

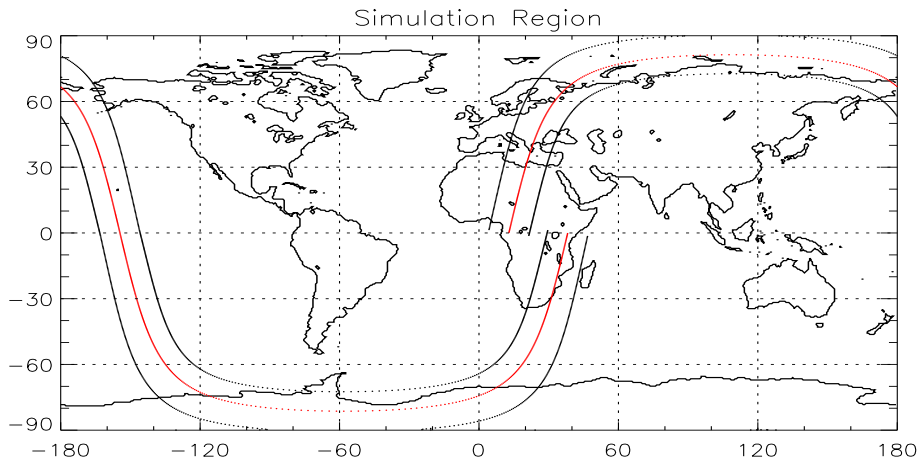


Figure 2: Simulated quasi-realistic swath of the IASI instrument. The red line delineates the suborbital track for which retrieval performance examples are shown.

The simulation study was done under clear air conditions. One topic we are focusing on is to show the equivalence of the retrieval results when performing the channel selection scheme on a climatology versus applying the same procedure on the forecast field (see Fig. 3, for temperature, Fig. 4, for SST, Fig. 5, for humidity, and Fig. 6, for ozone). Another aspect highlighted is the comparison of the two different channel selection methods outlined in subsection *Channel reduction procedure* for three different sets of numbers of channels (see Fig. 7).

## Temperature Results

In general we can see that the bias arising in the stratospheric *a priori* data (left panel of Fig. 3) could mostly be deleted by the inclusion of information from the IASI instrument (see middle and right panel of Fig. 3).

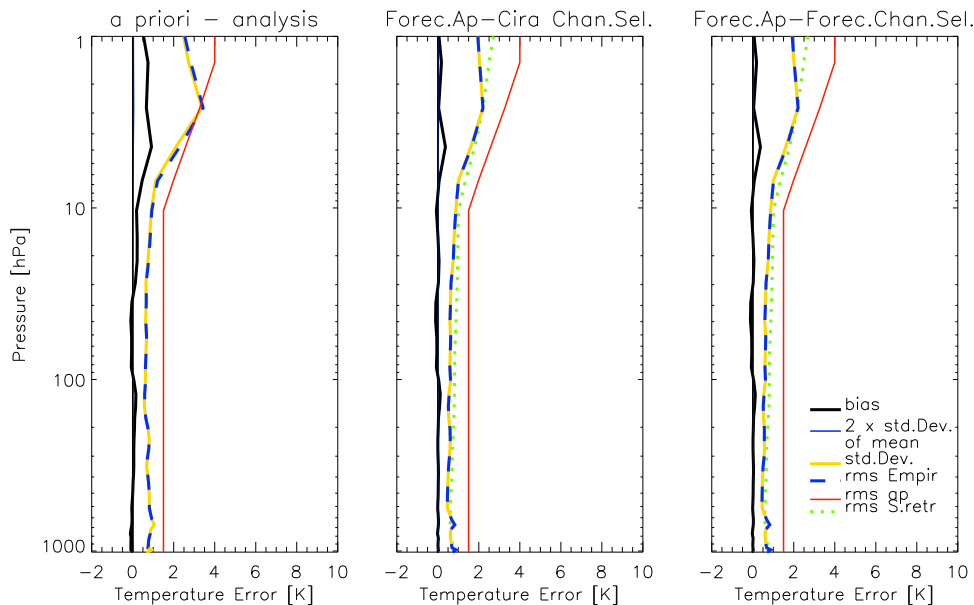


Figure 3: *A priori* minus "true" data and error statistic data for temperature profiles for two different initial data sets. Left panel: 24-hour forecast minus "true" data for temperature; middle panel: retrieval results for 24-hour forecast data for temperature and humidity profiles combined with *a priori* data consistent with the *a priori* error covariance matrices for ozone profiles and SST as first guess and the CIRA86aQ climatology (Kirchengast et al., 1999) with suitable ozone profiles obtained from U. S. standard profiles used for the channel selection process; right panel: the same first guess as in the middle panel but using the forecast data themselves (except for ozone where us. std. profile data were used) for the channel selection process. Legend: bias (black line), 2 times standard deviation of bias (solid blue line), standard deviation (yellow line), rms (dashed blue line), theoretical estimate of the rms of the finally accepted best state estimate (dotted green line), diagonal elements of the *a priori* error covariance matrices (red line).

A further comparison of the middle and the right panel of Fig. 3 which has the equivalent meaning of the comparison of the retrieval results for two different data sets used in the channel selection process points out that the differences only occur in the second digit. Since the usage of the climatology for the channel selection process is much more efficient than using the forecast data, because we have to select the channels only once (in comparison to a successive selection in the case of using the forecast data), we strongly suggest to perform the selection of channels used in the retrieval process on a climatology rather than on forecast data.

## Sea Surface Temperature Results

A closer examination of Fig. 4 shows that the retrieval exhibits better results for the rms than the theoretical estimate proposes. This can be explained by the fact that the retrieval of SST is highly dependent on the retrieval of the overlying atmosphere. Comparing the error analysis data of the SST only retrieval (c. f. Fig. 4, (c)) with the results from the joint temperature, humidity, ozone, and SST retrieval (c. f. Fig. 4, (a-b)) the latter shows a significantly improved performance – including that empirical rms data are quite consistent with the theoretical estimate whereas the SST only retrieval exhibits a small bias and deviations of the results which are almost as large as the ones used at input. On a closer examination of the error analysis data of the single SST retrieval (i. e., splitting it up into low, mid, and high latitudes) we find that the reason for these large errors lies in the tropics, more precisely, in regions with warm sea surface temperature. The main physical reason behind this is the significant water vapor continuum absorption over warm tropical oceans even in the "atmospheric window" channels (e. g., (Liou, 2002)).

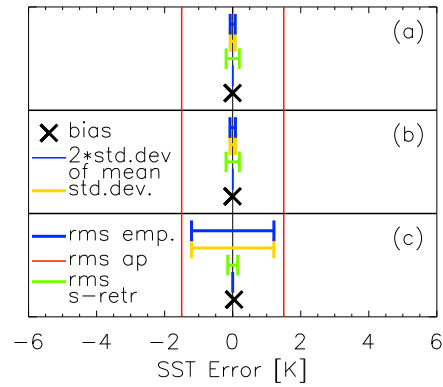


Figure 4: Error statistic data for SST for three different sets: The initial dataset of panel (a) corresponds to the middle panel of Fig. 3, panel (b) corresponds to the right panel of Fig. 3, whereas panel (c) is, in contrast to the temperature plot, the result of an SST only retrieval.

## Humidity Results

Comparing the results of the retrieved humidity when using the joint algorithm (see Fig. 5) mostly the same can be said as in the case of the estimation of temperature. We once more recognize that the resulting rms for the middle and the right panel of Fig. 5 is better than the theoretical estimate of it and once more the results for the different profile sets used in the channel selection process are quite the same.

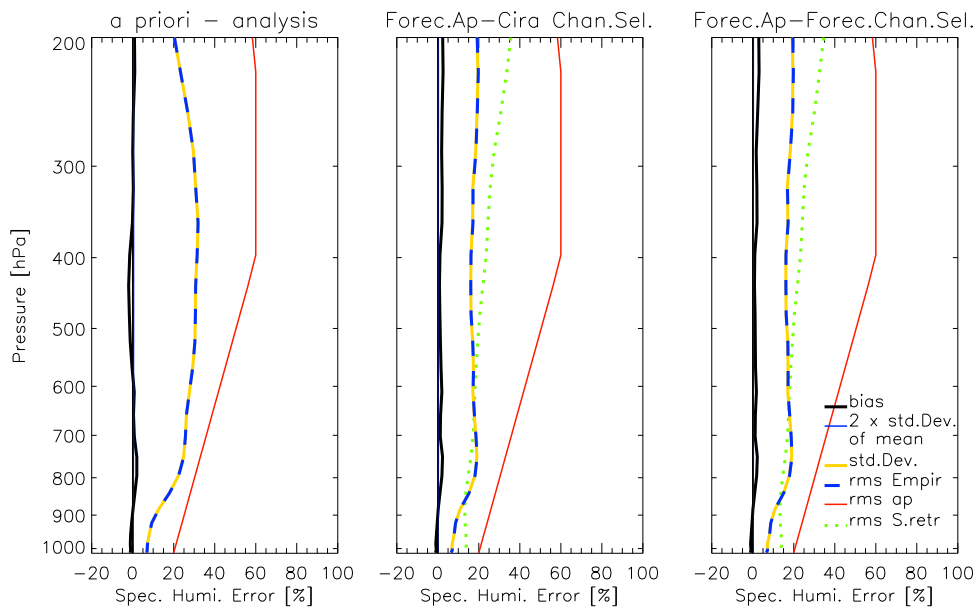


Figure 5: *A priori* minus "true" data and error statistic data for humidity profiles for two different initial data sets. Panel setup and legend corresponds to Fig. 3

We tested also a joint temperature-humidity profile retrieval targeted to the between 200 hPa and 500 hPa, a region of special interest to us, in order to check whether the estimated humidity becomes better and processing significantly faster because of a more limited channel selection for this region. It turned out, however, that this upper-troposphere-focused approach was very moderately faster and, in particular, the retrieval performance somewhat degraded.

## Ozone Results

Fig. 6 indicates that we get improvements of the ozone data only in regions of high concentration of ozone ("ozone layer") due to the fact that the weighting functions of ozone exhibit important peaks only at this height. Just like in the case of temperature and humidity the results for the different profile sets used in the channel selection process are quite the same. In addition, it was found that the results for temperature, humidity, and SST are quite independent from the initial guess of the ozone data if it remains in the domain of linearity or moderate non-linearity, respectively (a few 10% uncertainty level). This is also true vice versa.

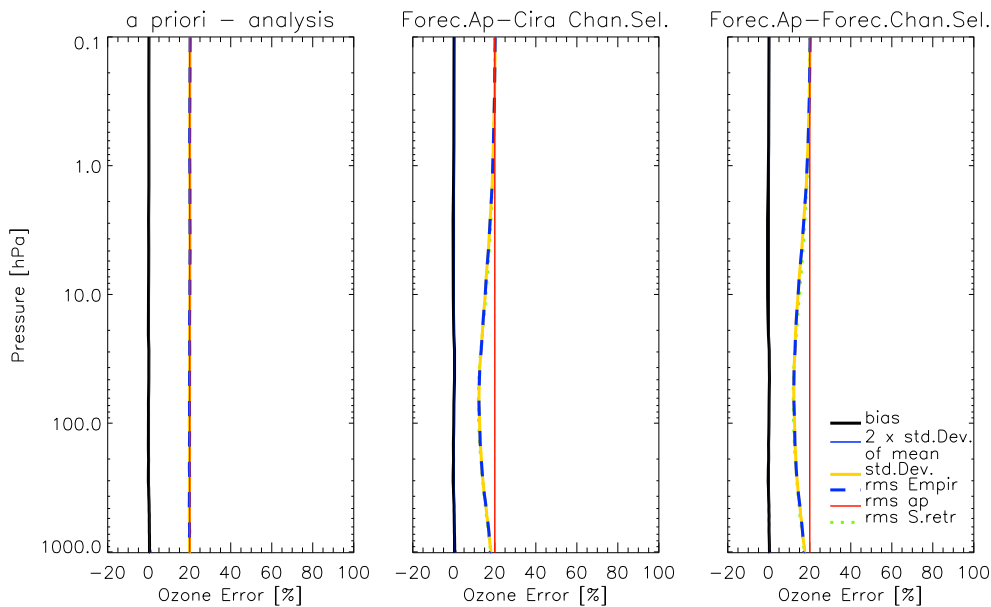


Figure 6: *A priori* data and error statistic data for ozone profiles for two different initial data sets. Panel setup and legend corresponds to Fig. 3.

## Channel Selection Results

As initial input set for all six cases we used an *a priori* data set which consists of data consistent with the *a priori* error covariance matrices for temperature, humidity, ozone, and SST. The three different sets of numbers of selected channels were chosen to get approximately 3.5%, 10% and 20% of the full number of IASI channels which resulted in an averaged number of selected channels per profile of 300 channels (smallest dataset), 887 channels (medium dataset), and 1808 channels (largest dataset).

An intercomparison of the temperature results (c. f. Fig. 7) shows that the theoretical estimation of the rms is decreasing slightly with increasing number of selected channels. This is not the fact for the empirical rms which is virtually the same for the small and the medium set but increases significantly for the case of  $\sim 1800$  selected channels. Furthermore, the maximum set of selected channels results in the appearance of slight bias structures which are not present in the two other sets resulting from the beginning of numerical instabilities of the implemented inversion scheme (large matrices). A comparison of the two different channel selection methods (IC, top three panels of Fig. 7 and MS, bottom three panels of Fig. 7) yields no significant difference for the cases with the small and the medium number of selected channels, only the set with 1808 selected channels shows a slightly better performance in the IC case which can be traced back to the fact that the IC theory selects fewer linearly dependent channels.

In summary we can say that these results suggest that the simpler MS channel selection approach, in the case of using a climatology for the selection of the used channels has the same efficiency as the IC method and closely similar performance. Tentatively the IC results are slightly better, presumably due



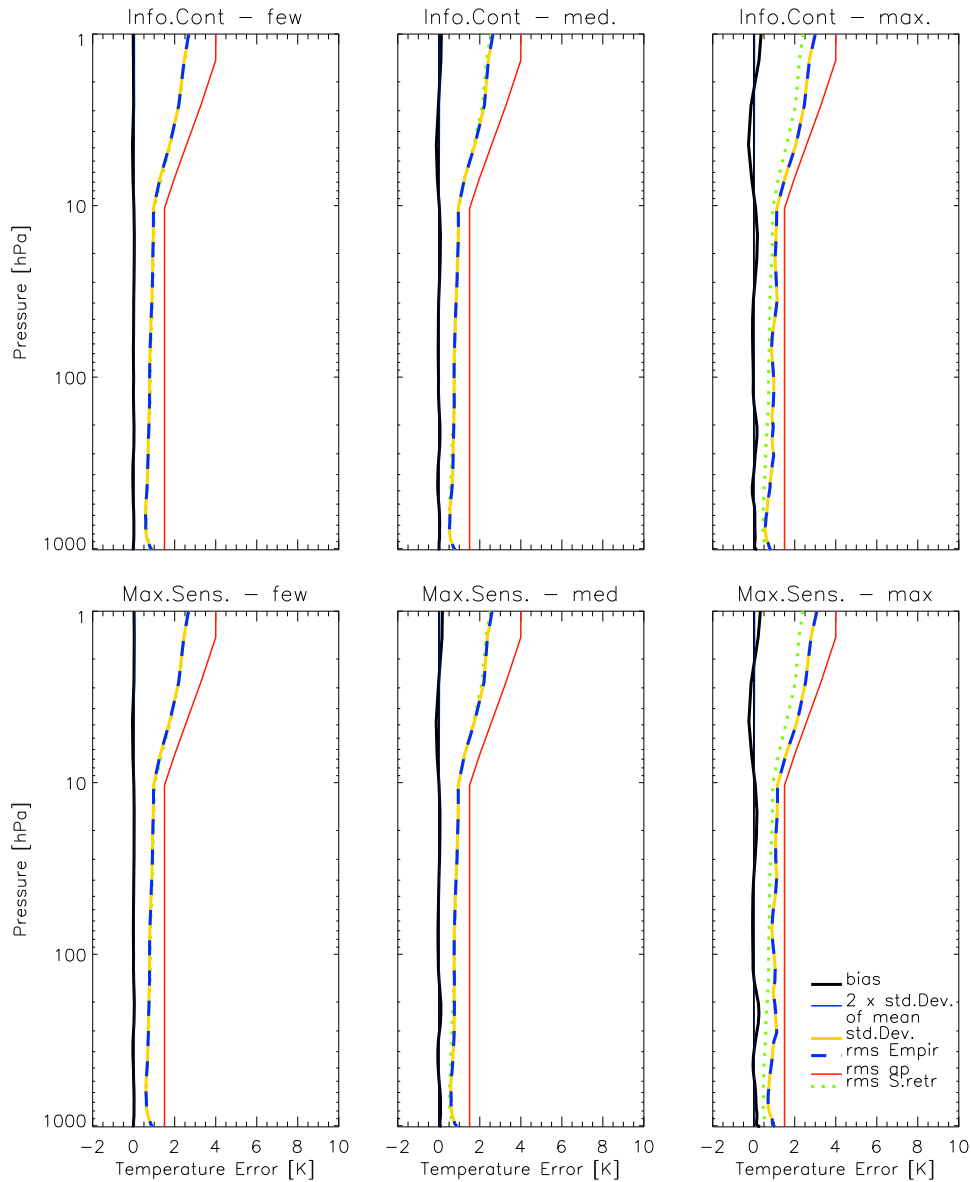


Figure 7: Panel layout as for Fig. 3 (see that legend). Explanation see text.

to the more even distribution of the selected channels over height, so the IC selection seems generally preferable.

## Summary and Outlook

We presented a retrieval algorithm for determining temperature, humidity and SST from radiance measurements made by the IASI instrument, scheduled for launch on-board of the METOP weather satellite series (first satellite to be launched in 2006). Main features are a sensible channel reduction procedure followed by an iterative optimal estimation retrieval. The channel reduction algorithm based on the information content theory makes the retrieval efficient – the procedure results in a reduction of the number of channels from more than 8400 to about 3.5% only ( $\sim 300$  channels). The retrieval performance does not significantly degrade due to this reduction. We also showed that the joint algorithm leads to a clearly improved performance compared to more specific retrieval setups, such as temperature-only or SST-only, etc., retrievals.

We obtain a retrieval accuracy of about 1 K in temperature and 15% to 20% up to  $\sim 400$  hPa in humidity, which is decreasing to about 35% at 200 hPa in humidity with a vertical resolution of 1 km to 3 km in the troposphere. For the stratosphere we found that *a priori* data exhibit important influence. Some challenging areas arose in the mid-latitude regions and at heights with weak sensitivity of the weighting functions (e.g., the tropopause). For ozone, the best estimate lies near 10% at a height of about 60 hPa but shows almost no difference to the assumed *a priori* error at heights lower than 400 hPa or higher than 5 hPa.

The results of this study provide guidance for further advancements. Our current and future work plan includes improvements of the *a priori* covariance matrices for temperature and humidity and the extension of the joint algorithm to other atmospheric species via an upgrade of the used forward model.

As a future step towards real data, the algorithm will then be applied to AIRS (Advanced Infrared Radiation Sounder) data, where our domain of particular interest is the upper troposphere and its climatic variability in humidity and temperature.

## Acknowledgments

We thank E. Weisz (SSEC, Univ. of Wisconsin, Madison, WI, U.S.A.) for valuable discussions on retrieval methodology and U. Foelsche (IGAM, Univ. of Graz, Austria) for support with acquisition of ECMWF fields. The work of M. S. was financed by the START research award of G. K., financed by the Austrian Ministry for Education, Science, and Culture and managed under Program No. Y103-N03 of the Austrian Science Fund.

## References

- Collard, A. D. (1998). Notes on IASI Performance. *U. K. MO Forecasting Research Technical Report No. 256*.
- Kirchengast, G., Hafner, J., and Poetzi, W. (1999). The CIRA86aQ\_UoG model: An extension of the CIRA-86 monthly tables including humidity tables and a Fortran95 global moist air climatology model. Technical Report for ESA/ESTAC No. 8/1999, IGAM, University of Graz, Austria.
- Lerner, J. A., Weisz, E., and Kirchengast, G. (2002). Temperature and humidity retrieval from simulated Infrared Atmospheric Sounding Interferometer (IASI) measurements. *Journal of Geophysical Research*, 107:10.1029/2001JD900254.
- Liou, K. N. (2002). *An Introduction to Atmospheric Radiation*. Oxford University Press, Oxford.
- Liu, X., Zaccheo, T. S., and Moncet, J.-L. (2000). Comparison of Different Non-Linear Inversion Methods for Retrieval of Atmospheric Profiles. In *Proceedings of the 10<sup>th</sup> Conference of Satellite Meteorology*, pages 293–295, Long Beach, California.
- Matricardi, M. and Saunders, R. (1999). A Fast Radiative Transfer Model for Simulation of Infrared Atmospheric Sounding Interferometer Radiances. *J. Appl. Optics*, 38:5679–5691.
- Rieder, M. and Kirchengast, G. (1999). Physical-statistical retrieval of water vapor profiles using SSM/T-2 sounder data. *Geophys. Res. Lett.*, 26:1397–1400.
- Rodgers, C. D. (2000). *Inverse Methods for Atmospheric Sounding: Theory and Practice*. World Scientific, Singapore.
- Sherlock, V. J. (2000). Results from the first U. K. MO IASI Radiative Transfer Model Intercomparison. *Forecasting Research Technical Report No. 287*.
- Weisz, E., Kirchengast, G., and Lerner, J. A. (2003). An efficient channel selection method for Infrared Atmospheric Sounding Interferometer data and characteristics of retrieved temperature profiles. Technical Report Wissenschaftl. Ber. No. 15, IGAM, University of Graz, Austria.